Proceedings

Geohazards

Engineering Conferences International *Year* 2006

Instrumental Intensity Scales for Geohazards

Steven Kramer* Sarah B. Upsall†

*University of Washington, kramer@u.washington.edu

†Department of Civil and Environmental Engineering, University of Washington, spaulsen@u.washington.edu

Instrumental Intensity Scales for Geohazards

Steven L. Kramer and Sarah B. Upsall

Department of Civil and Environmental Engineering, University of Washington, Box 352700, Seattle, Washington, 98195; PH: (206)685-2642; FAX (206)543-1543; Email: kramer@u.washington.edu, spaulsen@u.washington.edu

Abstract

The relationship between ground motion characteristics and geohazard-related earthquake damage was investigated for slope instability, lateral spreading, settlement, and buried pipeline damage, and the results used to develop two instrumental intensity scales. The scales are based on three velocity-related ground motion parameters that reflect the amplitude, frequency content, and duration of a ground motion. The scales provide intensity values that are strongly correlated to potential damage – one scale expresses intensity on a 0-10 scale and the other in terms of an apparent earthquake magnitude. The former is expected to be particularly useful for rapid identification of potential damaged areas using existing ShakeMap technology.

Introduction

Earthquake intensity scales, such as the Rossi-Forel, Modified Mercalli (MMI), and European macroseismic scales, have historically been based on qualitative observations of the effects of earthquake shaking. Instrumental intensity scales, on the other hand, can be used to describe ground motion levels quantitatively on the basis of actual strong motion recordings. In many areas, strong motion networks provide relatively dense spatial coverage so that strong motion records are available shortly after an earthquake. Such records can be used to determine intensity at the location of the recording, and also used with interpolation schemes to estimate ground motion intensity at other locations. The results of such exercises can be used to produce ground motion intensity maps, referred to as ShakeMaps (Wald et al., 1999a) in the United States, within minutes after earthquake shaking has ended. ShakeMaps can be used to direct emergency response and recovery resources in an efficient manner, and to better understand observed damage patterns. They can also be generated for different anticipated scenario events to aid in emergency planning and hazard mitigation.

Earthquake geohazards result from several different physical mechanisms, each of which is influenced by different characteristics of an earthquake ground motion. For the purpose of this investigation, earthquake geohazards were grouped into the following four categories:

1. *Slope Instability* – permanent deformation of slopes due to inertial forces generated by strong ground motion. This category refers to slopes comprised of soils that maintain the great majority of their strength during earthquake shaking, i.e. that behave in a ductile manner.
2. *Lateral Spreading* – lateral deformation of slopes in potentially liquefiable soils that develop due to pore pressure-induced softening and/or weakening of the soil

during earthquake shaking. Flow slides, the deformations of which are driven by static rather than dynamic stresses, are not included in this category.

3. *Settlement* – vertical ground surface displacement of potentially liquefiable soil profiles that develop with the dissipation of earthquake-induced pore pressures. Settlements of unsaturated soils, which can be significant in some cases but are usually less common and smaller than the previously described settlements, are not included in this category.
4. *Buried Pipeline Damage* – breakage of pipelines and/or pipe joints due to transient ground deformations. This category does not include pipeline damage caused by ground failure (e.g. slope instability or liquefaction).

Each of these mechanisms can lead to significant and widespread earthquake damage that can threaten public safety and the economic well-being of a particular region. The extent to which each actually develops depends on the level of earthquake ground shaking and on the level of vulnerability of the geologic environment. The research described in this paper is intended to address the former of these issues by identifying the ground motion characteristics most closely related to each of these damage mechanisms, and then using those ground motion characteristics to describe damage to vulnerable infrastructure elements.

Vulnerability

Observational intensity scales implicitly consider the vulnerability of a particular environment by relating the intensity to the response of different types of structures (e.g. rocking motor cars, ringing bells, performance of "well-built ordinary structures," etc. in the MMI scale) in that environment. Instrumental intensity scales, on the other hand, are based on ground shaking characteristics alone; the damage associated with a particular instrumental intensity value will depend on the vulnerability of the environment subjected to that level of shaking. In order to "anchor" an instrumental intensity scale to some measure of damage, the scale must be calibrated in some way. The ShakeMap intensity (SMI) scale of Wald et al. (1999b), which is based on a combination of peak acceleration (at low to moderate shaking levels) and peak velocity (at high shaking levels), was calibrated against MMI (Table 1).

Table 1. SMI intensity scale (after Wald et al., 1999a)

Perceived Shaking	Not felt	Weak	Light	Moderate	Strong	Very strong	Severe	Violent	Extreme
Potential Damage	none	none	none	Very light	Light	Moderate	Moderate/ Heavy	Heavy	Very heavy
PGA (%g)	< 0.17	0.17-1.4	1.4-3.9	3.9-9.2	9.2	18-34	34-65	65-124	> 124
PGV (cm/sec)	< 0.1	0.1-1.1	1.1-3.4	3.4-8.1	8.1-16	16-31	31-60	60-116	> 116
Instrumental intensity	I	II – III	IV	V	VI	VII	VIII	IX	X+

In an attempt to produce an instrumental intensity scale related to physical damage, the scales described in this paper were developed using computational

response models instead of empirical response observations – the intent was to use advances in understanding and modeling of geotechnical response to identify the characteristics of ground motions that most strongly influence response, and therefore damage. These analyses required specification of an "inventory" of vulnerable systems with some potential to be damaged by earthquake shaking. For slope instability damage, the inventory was assumed to be consistent with a population of engineered slopes. Lateral spreading and settlement of potentially liquefiable soils frequently occurs in unimproved natural soils found in coastal areas of urban environments (near bridges, port facilities, etc.); the inventories used for these mechanisms were taken to be consistent with the average conditions from databases of lateral spreading case histories (Youd et al., 2002) and post-liquefaction settlement case histories (Wu, 2002). Buried pipeline inventories were taken as the average of those published by the American Lifeline Alliance (American Lifeline Alliance, 2001).

Intensity Scale Framework

The Pacific Earthquake Engineering Research Center (PEER) has developed a framework for performance-based earthquake engineering. The PEER framework describes ground motions in terms of an intensity measure (*IM*), which is simply a quantitative descriptor of the level of shaking. The level of response of a physical system to that intensity measure is described by an engineering demand parameter (*EDP*). The physical damage associated with that level of response is described by a damage measure (*DM*). Therefore, we can establish relationships between the variables by means of response functions and damage functions, as illustrated in Figure 1. In order to predict damage as accurately as possible, *IM*s that correlate well to *EDP*s and *EDP*s that correlate well to *DM*s must be identified.

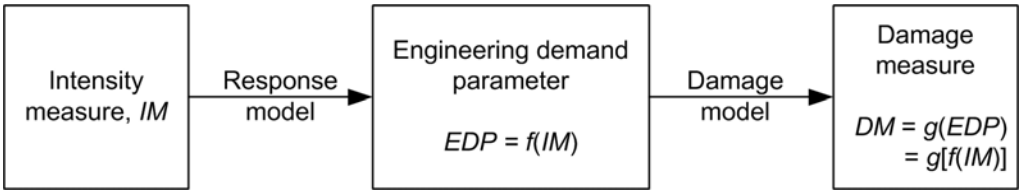

Figure 1. Schematic illustration of intensity scale framework.

The efficiency of an *IM* can be expressed in terms of the dispersion of *EDP*|*IM* or *DM*|*IM*. Efficient *IM*s are those with low conditional uncertainty, i.e. *IM*s that are closely related to response and/or damage. For each of the damage mechanisms described in this paper, an extensive search for an efficient *IM* was undertaken. The identified *IM* was then used to predict *DM* for that damage mechanism. The *DM*s from the individual damage mechanisms were then combined to form a composite *DM*, which was then used as the basis for a geohazard intensity scale.

Response Models

A series of response models were used to predict *EDP*s from *IM*s. For the slope stability problem, permanent displacements were computed using a Newmark sliding block model, which is capable of reflecting the influence of ground motion amplitude, frequency content, and duration on permanent displacements of ductile slopes. Lateral

spreading displacements were computed using a one-dimensional, nonlinear, effective stress-based site response analysis with the capability of considering initial shear stresses. The site response analysis was calibrated so that the mean predicted permanent displacement for a suite of ground motions matched the mean permanent displacement predicted by available empirical lateral spreading models. Post-liquefaction settlements were computed from excess pore pressure ratios and maximum shear strains computed by one-dimensional, nonlinear, effective stress-based site response analysis using the procedure of Shamoto and Zhang (1998). Buried pipeline response was computed using the model developed by the American Lifeline Alliance, which was calibrated to represent average pipeline characteristics from inventory data for San Francisco and Los Angeles.

Damage Models

To compare the levels of physical damage associated with the various levels of response induced in slopes, liquefiable soil profiles, and buried pipelines, a common measure of physical damage was required. To accomplish this, a semantically-derived damage scale was developed. The scale assigns numerical values to five levels of physical damage – negligible, slight, moderate, severe, and catastrophic – as indicated in Table 2.

Table 2. Definition and description of damage measures.

Level	*DM*	Description
Negligible	0.0 – 0.1	No loss of functionality; insignificant repair cost
Slight	0.1 – 0.4	Brief loss of functionality; minor repair cost
Moderate	0.4 – 0.7	Brief to minor loss of functionality; moderate repair cost
Severe	0.7 – 0.9	Substantial loss of functionality; repair costs approach value
Catastrophic	0.9 – 1.0	Complete loss of functionality; repair costs exceed value

The *EDP* levels associated with these *DM* ranges were developed by polling a group of engineers experienced in local (Seattle, Washington) practice and a group with significant international experience in post-earthquake reconnaissance investigations. These engineers were asked for their opinions on the levels of lateral and vertical displacement associated with each damage level. The results of these surveys were used to develop the damage models illustrated in Figure 2.

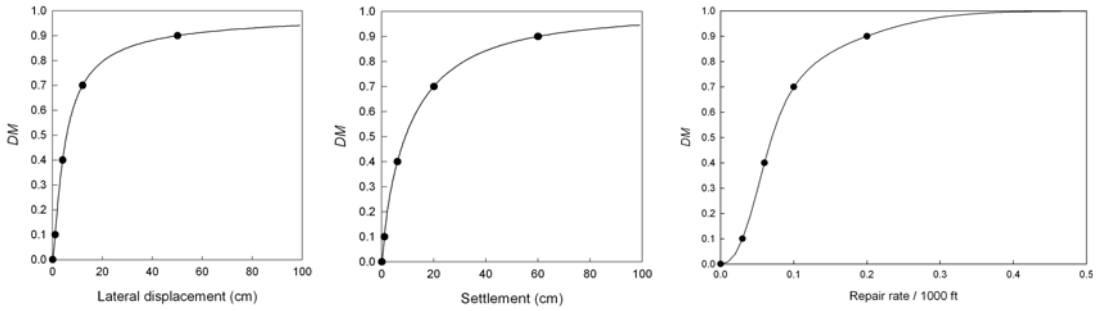

Figure 2. Graphical illustration of damage models: (a) slope instability and lateral spreading, (b) settlement, and (c) buried pipeline damage. Solid circles mark boundaries between different damage levels.

Development of Hazard Scales

The hazard scale development process for each potential damage mechanism involved (a) combination of the response and damage models to allow *DM* to be computed directly from *IM*, (b) identification of the *IM* that most efficiently predicted *DM*, and (c) establishment of the *IM-DM* relationship. The composite geohazard intensity scale required combination of the individual damage mechanism components and interpretation in the context of attenuation behavior.

Slope Stability Component

Previous research by Travasarou and Bray (2003) identified Arias intensity (Arias, 1970) as an efficient *IM* for slope failures involving little dynamic response of the material above the failure plane (i.e. shallow failures and/or deeper failures in relatively stiff material). Defining the *EDP* as the mean permanent displacement from sliding block analyses performed using 360 one-degree-incremental components of each motion, and using a database of 455 motions, an *IM* defined as $IM_{slope} = 0.7I_{a,1} + 0.3I_{a,2}$, where $I_{a,1}$ and $I_{a,2}$ are the higher and lower of the two recorded components, respectively, was found to produce the best fit to *DM*. By weighting the contributions from each of ten slopes (normally distributed with $\mu_{FS} = 1.5$ and $\sigma_{FS} = 2$) according to their probabilities, a model of the form

$$DM_{slope} = \left[\frac{0.0150IM_{slope}^{1.9955}}{1+0.0150IM_{slope}^{1.9955}}\right]^{0.1969}\left(1+\left(\frac{1.5679}{IM_{slope}}\right)^{2.1811}\right)^{-0.5} \quad (1)$$

was developed. The model is illustrated in Figure 3.

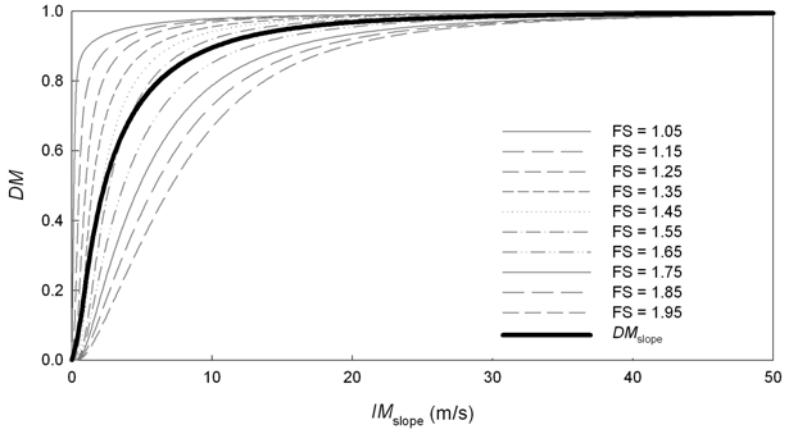

Figure 3. Variation of DM_{slope} with IM_{slope} for various initial factors of safety, and for weighted average of all initial factors of safety.

Lateral Spreading Component

Kramer and Mitchell (2006) showed that an intensity measure known as CAV_5 was an efficient predictor of pore pressure generation in liquefiable soils. CAV_5 is defined as cumulative absolute velocity (Benjamin and Associates, 1988) calculated with a threshold acceleration of 5 cm/sec2. CAV_5 was found to also be an efficient predictor of lateral spreading displacement in analyses performed in this research. Considering components resolved at 120 three-degree incremental directions for each of 455

motions, an *IM* defined as $IM_{LS} = \sqrt{CAV_{5,1}^2 + CAV_{5,2}^2}$ where $CAV_{5,1}$ and $CAV_{5,2}$ are the higher and lower values of the measured components, respectively, was found to produce the best fit to *DM*. The resulting model can be expressed as

$$DM_{LS} = \left[\frac{(0.00033 IM_{LS}^{0.91556})}{(1 + 0.00033 IM_{LS}^{0.91556})} \right]^{0.04273} \left[1 + \left(\frac{353.804}{IM_{LS}} \right)^{4.06479} \right]^{-0.5} \quad (2)$$

Settlement Component

CAV_5 was also found to also be an efficient predictor of lateral spreading displacement in analyses performed in this research. Considering components resolved at 120 three-degree incremental directions for each of 455 motions, an *IM* defined as $IM_{sett} = \sqrt{CAV_{5,1}^2 + CAV_{5,2}^2}$ where $CAV_{5,1}$ and $CAV_{5,2}$ are respectively the higher and lower values of the measured components was found to produce the best fit to *DM*; therefore, $IM_{\text{sett}} = IM_{\text{LS}}$. The resulting model can be expressed as

$$DM_{sett} = \left[\frac{(0.000156 IM_{sett}^{1.3296})}{(1 + 0.000156 IM_{sett}^{1.3296})} \right]^{0.7822} \left[1 + \left(\frac{0.051549}{IM_{sett}} \right)^{17.7345} \right]^{-0.5} \quad (3)$$

Buried Pipeline Component

Peak ground velocity has been identified by the American Lifeline Association as the *IM* to which pipeline damage rates are most closely related. Using the 455 motions in the ground motion database, a model for pipeline damage can be expressed as

$$DM_{pipe} = \left[\frac{10000(0.000648 PGV)^{7.9836}}{1 + 10000(0.000648 PGV)^{7.9836}} \right]^{0.0266} \left[1 + \left(\frac{97.4184}{PGV} \right)^{4.1146} \right]^{-0.5} \quad (4)$$

Composite Geohazard Damage Measure

A composite geohazard-related intensity scale was developed by weighting each of the four previously described scale in proportion to their anticipated contributions to total damage in typical urban environments. It should be noted that actual damage depends on vulnerability, and that the indicated intensity is representative of damage in regions with inventories of vulnerable systems similar to that assumed herein. For example, the indicated instrumental intensities are likely to overstate the damage potential of ground motions in regions that do not have liquefiable soils. A small group of people experienced in loss estimation and earthquake reconnaissance were polled to obtain information used to develop weighting factors for the different damage mechanisms. This information was used to develop the following composite geohazard intensity scale

$$DM_{\text{geo}} = 0.3\, DM_{\text{slope}} + 0.2\, DM_{\text{LS}} + 0.2\, DM_{\text{sett}} + 0.3\, DM_{\text{pipe}} \quad (5)$$

Geohazard Intensity Scales

The preceding DM_{geo} values were used to develop two geohazard intensity scales. The first, known as the Geohazard Damage Potential Intensity, DPI, is obtained by scaling DMgeo by a factor that simply maps its values to a 10-point scale, i.e.

$$DPI_{geo} = 10\, DM_{geo} \tag{6}$$

The second scale was developed by fitting the form of a relatively simple ground motion attenuation relationship to a strong motion database for a reference site condition, and then inverting the attenuation relationship to express the intensity in terms of an "apparent" magnitude value corresponding to a standard reference distance on the standard reference site condition. Selecting "soft rock" as the reference site condition and using a reference distance of 25 km, the Geohazard Intensity can be expressed as

$$I_{geo} = \frac{6.6138}{\left(-\ln DM_{geo}\right)^{0.10649}} \tag{7}$$

The value of I_{geo} can be interpreted as the earthquake magnitude expected to cause an equivalent amount of geohazard damage at a rock site located at an epicentral distance of 25 km. It should be noted that tis expression has an effective "floor" of $I_{geo} \approx 5.5$, which follows from the fact that ground motions equal to or weaker than those expected at a rock site 25 km from a $M = 5.5$ earthquake are not expected to cause geohazard-related damage. As a result, use of the Geohazard Intensity scale is not recommended for events with magnitudes less than 6.

The proposed intensities were used in a procedure similar to that described by Wald et al. (1999a) to develop instrumental intensity maps for recent earthquakes. Figure 4 shows the results of such procedures for the southern portion of the San Francisco Bay Area in the 1989 Loma Prieta ($M = 6.9$) earthquake. The intensity values can be seen to generally decrease from south to north, which is consistent with the fact that the epicenter of the earthquake was south of the mapped area, and to be locally increased in the areas adjacent to San Francisco Bay which are known to be underlain by soft soils. DPI_{geo} values are primarily in the range of 1 – 3, indicating slight damage with a region of moderate damage indicated for the southeast portion of the map; this distribution is generally consistent with observed damage patterns.

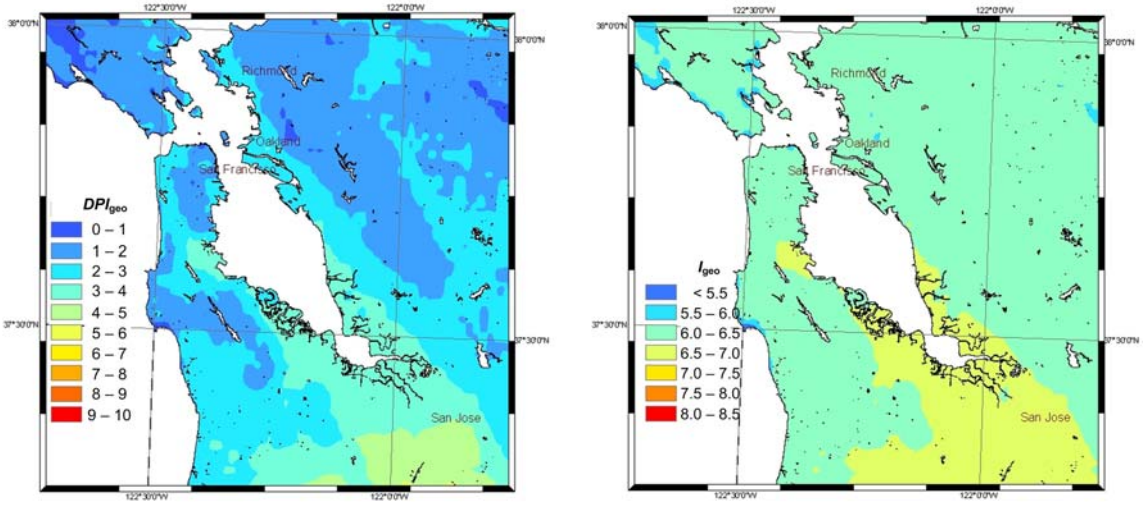

Figure 4. Illustration of (left) Geohazard Damage Potential Intensity, DPI_{geo}, and (right) Geohazard Intensity, I_{geo}, for the 1989 Loma Prieta earthquake.

Conclusions

An investigation of the effects of ground motion characteristics on geohazard potential showed that damage was more closely correlated to velocity-related parameters such as *PGV*, Arias Intensity, and CAV_5 than to the higher-frequency parameter (*PGA*) relied upon in commonly used instrumental intensity scales. Calculation of instrumental intensity using the proposed scales is expected to provide an improved indication of the damage potential of earthquake ground motions.

References

American Lifeline Alliance (2001). *Seismic Fragility Formulations for Water Systems*, ASCE, Reston, VA.

Arias, A. (1970). "A measure of earthquake intensity," *Seismic design for nuclear power plants*, R.J. Hansen, ed., The MIT Press, Cambridge, MA, pp. 438-483.

Benjamin, Jack R. and Associates (1988). "A criterion for determining exceedance of the Operating Basis Earthquake," *EPRI Report NP-5930*, Electric Power Research Institute, Palo Alto, California.

Kramer, S.L. and Mitchell, R.A. (2006). "An Efficient and Sufficient Scalar Intensity Measure for Soil Liquefaction," *Earthquake Spectra*, Vol. 22, No. 2, pp. 1-26.

Shamoto, Y. and Zhang, J. (1998). "Evaulation of Seismic Settlement Potential of Saturated Sandy Ground Based on Concept of Relative Compression," Special Issue of Soils and Foundations, Japanese Geotechnical Society, p. 57-68

Shamoto, Y., Sato, M, and Zhang, J. (1996). "Simplified estimation of earthquake-induced settlements in saturated sand deposits," Soils and Foundations, Vol. 36, No. 1, pp. 39-50.

Travasarou, T. and Bray, J. (2003). "Optimal ground motion intensity measures for assessment of seismic slope displacements," *Proceedings,* 2003Pacific Conference on Earthquake Engineering, pp. 93-100.

Wald, D., Quitoriano, V., Heaton, T., and Kanamori, H, Scrivner, C., and Worden, C. (1999a). TriNet "ShakeMaps": Rapid Generation of Peak Ground Motion and Intensity Maps doe Earthquakes in Southern California, *Earthquake Spectra*, Volume 15, No. 3, p. 537-555.

Wald, D., Quitoriano, V., Heaton, T., and Kanamori, H. (1999b). Relationships between Peak Ground Acceleration, Peak Ground Velocity and Modified Mercalli Intensity in California, *Earthquake Spectra*, Volume 15, No. 3, p. 557-564.

Wu, J., (2002). "Liquefaction triggering and post liquefaction deformations of Monterey 0/30 Sand under uni-directional cyclic simple shear loading," *Ph. D. Dissertation*, University of California, Berkeley, 509 pp.

Youd, T.L., Hansen, C.M., and Bartlett, S.F. (2002). "Revised multilinear regression equations for prediction of lateral spread displacement", *Journal of Geotechnical and Geoenvironmental Engineering*, ASCE, 128(12), 1007-1017.